Journal of the Korean Society of
Agricultural Engineers, Vol. 39, 19~25
December 1997

Finite Element Numerical Analysis on Tidal Characteristic Changes due to Seadike Construction

Kwun, Soon Kuk* · Na, Jeong Woo · Chang, Hyun Jin*****

**College of Agriculture and Life Sciences, Seoul National University*
***Rural Development Corporation*
****Graduate School, Seoul National University*

Abstract □ The prediction of changes in the tidal regime due to the sea dike closure in the Saemankum area was performed using the nonlinear finite element model, TIDE. Based upon an overall comparison of calibrated model results with available field data, the TIDE model behaves well and is good representation of the hydrodynamic of the Saemankum tidal project area. It is shown that the TIDE model does an excellent job of computing the changes of tidal characteristics resulting in sea dike closure in an estuary area.

Keywords □ finite element model, shallow water equation, Galerkin's method, iterative solution.

I. Introduction

The tideland reclamation is vital to counterplan for increasing demand for the land and water resources in Korea. However, it is known that seadike construction for the tideland reclamation may significantly affect the water circulation system around the neighboring water body not only resulting in changes of the coastal geometry but also causing the environmental problems. Therefore, it is necessary that the resultant effects of seadike construction must be carefully assessed. In this study, it is intended to investigate the various effects due to the seadike construction by comparing the simulated tidal velocities and elevations before and after the construction of Saemankeum seadike.

The simulations were made by TIDE, which is a nonlinear two-dimensional harmonic model formulated by finite element method.

II. Description of the Model

1. Governing Equations

The equations used to describe tidal characteristics are the shallow water equations which are derived by integrating the continuity and momentum equations over depth, and are expressed as ;

$$\frac{\partial \eta}{\partial t}+\frac{\partial}{\partial x}[u(h+\eta)]+\frac{\partial}{\partial y}[v(h+\eta)]=0 \qquad (1)$$

$$\frac{\partial u}{\partial t}+u\frac{\partial u}{\partial x}+v\frac{\partial u}{\partial y}+g\frac{\partial \eta}{\partial x}$$

$$-fv-\frac{1}{\rho h}\left(\frac{h}{h+\eta}\right)(\tau_x^s-\tau_x^b)=0 \quad (2)$$

$$\frac{\partial v}{\partial t}+u\frac{\partial v}{\partial x}+v\frac{\partial v}{\partial y}+g\frac{\partial \eta}{\partial y}$$

$$+fu-\frac{1}{\rho h}\left(\frac{h}{h+\eta}\right)(\tau_y^s-\tau_y^b)=0 \quad (3)$$

where u and v are the depth averaged velocities in the x and y coordinate directions, respectively, η is surface elevation above mean water level, h is mean water depth, t is time, g is accleration due to gravity, ρ is the density of water, f is the Coriolis parameter, τ_x^s and τ_y^s are surface stresses and τ_x^b and τ_y^b are bottom stresses in the x and y directions, respectively.

2. Finite Element Formulation

The spatial dependence of the shallow water equations will be resolved by using the finite element method. Applying Galerkin's method, the weighted residual governing equations are obtained by weighting the associated errors with the residual elevation and velocities, and integrating over the interior domain.

The differential time dependence in finite element formulations are resolved by reducing them to sets of harmonic equations. Substituting into finite element formulations for each of the responses and load vectors, taking appropriate time derivatives and grouping terms lead to sets of time independent linear equations of the following type.

$$i\omega[M_\eta]\{\eta\}-[D]\{U\}=-\{P_\eta\}^{lin}+\{P_\eta\}^{nl} \quad (4)$$

$$i\omega[M_U]\{U\}+[M_F]\{U\}+[M_C]\{U\}$$
$$+g[D]^T\{\eta\}=\{P_W\}^{lin}+\{P_F\}^{nl}-\{P_C\}^{nl} \quad (5)$$

where $\{\eta\}$ is an elevation vector, $\{U\}$ is a velocity vector, $[M_\eta]$ is a continuity equation coefficient matrix, $[D]$ is a derivative matrix, $\{P_\eta\}^{lin}$ is a load vector for flux prescribed boundaries, $\{P_\eta\}^{nl}$ is a load vector for finite amplitude effects, $[M_u]$ is a momentum equation mass matrix, $[M_F]$ is a linearized frictional distribution matrix, $[M_C]$ is a Coriolis matrix, $\{P_W\}^{lin}$ is a wind stress loading vector, $\{P_F\}^{nl}$ is a load vector containing difference between linearized friction and full nonlinear friction, and $\{P_C\}^{nl}$ is a load vector containing convective acceleration effects.

3. Iterative Solution Procedure

The iterative solution starts out with the assumption that the nonlinear loadings are zero and $\{U\}$ can be expressed from equation (5).

$$\{U\}=[M_{tot}]^{-1}(\{P_W\}-g[D]^T\{\eta\}) \quad (6)$$

in which, $[M_{tot}]^{-1}=i\omega[M_U]+[M_F]+[M_C]$
Substituting for equation (6) into the associated continuity equation (4) as follows.

$$(i\omega[M_\eta]+g[D][M_{tot}]^{-1}[D]^T)\{\eta\}$$
$$=-\{P_\eta\}+[D][M_{tot}]^{-1}\{P_W\} \quad (7)$$

Hence $\{\eta\}$ is solved for using equation (7) and subsequently $\{U\}$ is solved for using equation (6).

Computed velocity and elevation are used for evaluating $\{P_F\}^{nl}$ and $\{P_C\}^{nl}$ which are added $\{P_W\}$ in equation (6) and compute

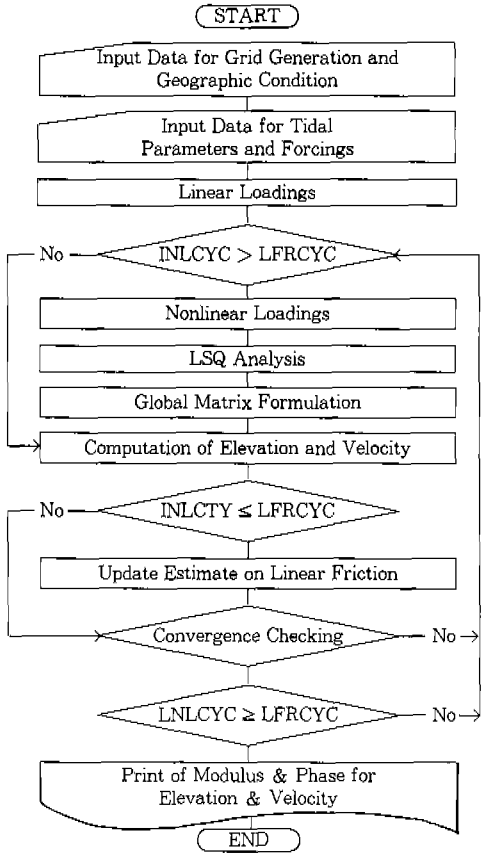

Fig. 1. Schematic flow chart with iterative solution procedure for the TIDE model

elevation and velocity repeatly until convergence within given values.

The iterative algorithm for the TIDE model would be shown in Fig. 1.

III. Model Calibration

The model calibrations are carried out on the area of huge Saemankeum Comprehensive Reclamation Project located at the western coast of Korea. The seadikes with its total length of 33km are under construction. This area covers the Dongjin and Mangyeong river basins in the east, Gogunsan islands in

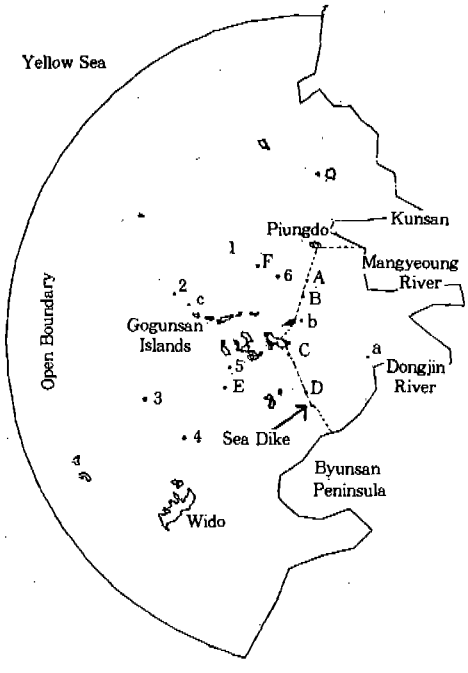

Fig. 2. Layout of Saemankeum project area and gauging site for model calibration

the west and Byunsan peninsula in the south as shown in Fig. 2.

A numerical mesh is designed to represent the Saemankeum Reclamation Project area including neighboring sea by using automatic mesh generator as shown in Fig. 3. The mesh consists of 948 elements and 532 nodes, that may allow the accurate representation of currents for the variation of tidal characteristics.

Current meter data for 6 locations at the neighboring area from the proposed sea dike line are available and obtained from the Rural Development Corporation (RDC) for the period of August 1993 and July 1995 as shown in Table 1.

Input data consist of water depth, friction factor, Coriolis factor and gravitational

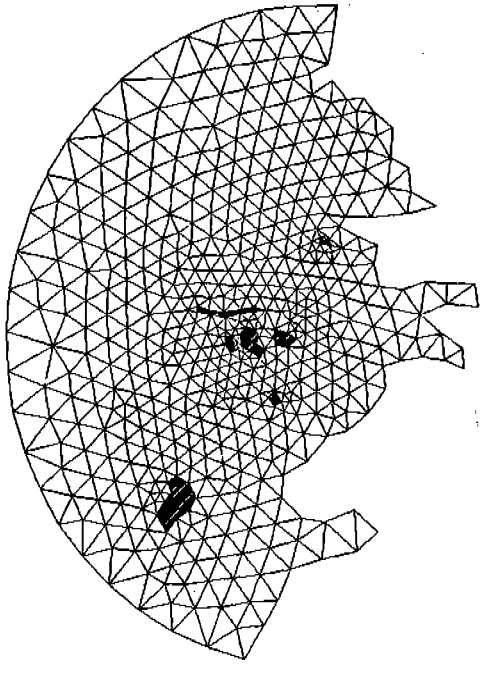

Fig. 3. Computational mesh for the Saemankeum project area

constant. The water depths and friction factors in each mesh are used for model calibration.

Boundary forcings in the TIDE model consist of 10 tide components (M_2, S_2, K_1, O_1, N_2, L_2, K_2, P_1, M_4, MS_4), freshwater inflow and winds. Freshwater inflows are prescribed at the river mouth of all major tributaries. As all of these flows are quite small, they are neglected. Wind factors are not included for the model calibration because of beyond of this study.

In the calibration phase, various model parameters may be adjusted within the limits of their uncertainties. For achieving the best results, it is necessary to compare with the measurement data.

Fig. 4 presents the comparisons between

Table 1. Tidal velocity and elevation measurement

Station	Location	Observation period	Remarks
A	35°54′19″N 126°30′32″E	1993. 8. 16. 00:00-24:00	Tidal velocity
B	35°53′01″N 126°30′24″E	1993. 8. 16. 00:00-24:00 1995. 7. 12. 00:00-24:00	
C	35°48′17″N 126°29′04″E	1993. 8. 16. 00:00-24:00	
D	35°45′05″N 126°31′07″E	1993. 8. 16. 00:00-24:00 1995. 7. 12. 00:00-24:00	
E	35°46′00″N 126°24′00″E	1995. 7. 12. 00:00-24:00	
F	35°54′30″N 126°26′30″E	1995. 7. 12. 00:00-24:00	
a	35°48′00″N 126°36′55″E	1993. 8. 16. 00:00-24:00	Tidal elevation
b	35°50′18″N 126°29′14″E	1993. 8. 16. 00:00-24:00	
c	35°51′30″N 126°19′00″E	1993. 8. 16. 00:00-24:00	

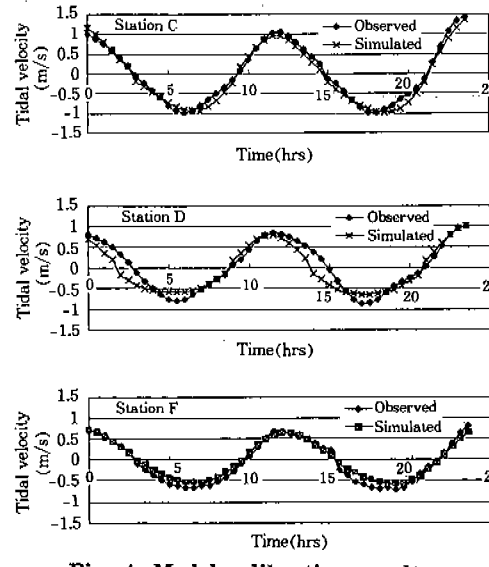

Fig. 4. Model calibration results

the simulated tidal velocity and observed one. Magnitude of the computed velocity agrees well with the observed data. Note that the magnitude and time of the maximum velocity are particularly in good agreement.

IV. Model Results

With the boundary forcings and the parameters calibrated previously, computations are made to see the effects in changing tidal characteristics due to the seadike closure. Computed tidal elevation, tidal velocity and short term pattern of flow circulations for six locations(stations 1, 2, 3, 4, 5 and 6 in Fig. 2) are compared between before and after the seadike closure. Due to space and time limitation, only a few of these results are presented.

1. Tidal Elevation

Fig. 5 presents the comparisons for the tidal elevation changes between before and after seadike construction during 24 hours on August 20, 1990. The maximum elevation differences at flood tide and ebb tide between before and after seadike construction are also presented in Table 2 on the same day. Considering that differences of tidal elevation changes due to the seadike construction are insignificant, we can conclude that there would be very little influence even in constructing a huge Saemankeum seadike. However, it is seen that the tidal ranges have the tendency of decreasing due to the maximum sea water level come down and minimum sea water level rise after seadike closure as shown in Table 2.

2. Tidal Velocity

Comparison of tidal current velocities between before and after seadike construction on August 20, 1990 for 6 locations are presented in Fig. 6 and Table 3. As was seen in

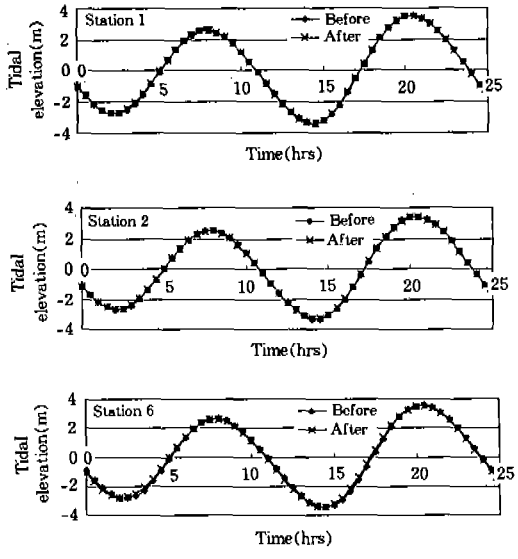

Fig. 5. Comparison of tidal elevation differences

Table 2. Tidal elevation at flood and ebb tide

Station	Flood tide(m)		Ebb tide(m)	
	Before	After	Before	After
1	3.51	3.50	-3.40	-3.39
2	3.42	3.38	-3.30	-3.28
3	3.31	3.28	-3.19	-3.17
4	3.34	3.32	-3.21	-3.22
5	3.46	3.40	-3.34	-3.30
6	3.57	3.50	-3.45	-3.41

the results of tidal elevation, tidal velocities betweeen before and after seadike closure shows only a little changes at the station 3 and 4. However, in the adjacent area to the proposed line of seadike such as station 5 and 6, tidal velocities are significantly reduced as shown in Fig. 6.

Current velocity vectors are presented for the comparison of current circulation pattern due to sea dike closure. Fig. 7 presents current velocity vectors at 18:00 for the flood tide on August 20, 1990.

Based upon an analysis of overall circula-

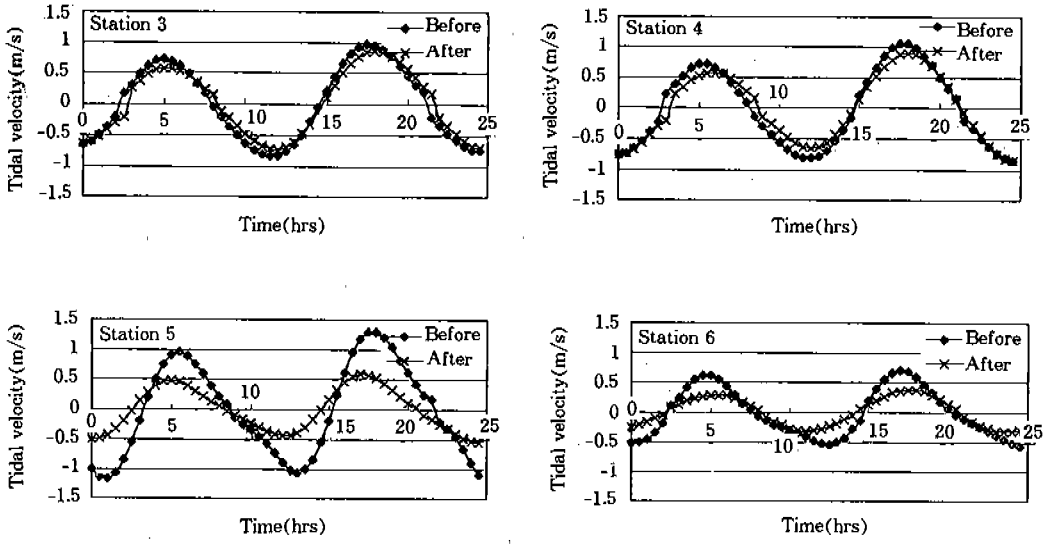

Fig. 6. Comparison of tidal velocity

Table 3. Tidal velocity at flood and ebb tide

Station	Flood tide				Ebb tide			
	Velocity(m/s)		Direction(°)		Velocity(m/s)		Direction(°)	
	Before	After	Before	After	Before	After	Before	After
1	0.85	0.71	19	38	0.74	0.66	202	218
2	1.24	1.13	58	82	1.01	0.89	232	250
3	0.97	0.85	27	47	0.74	0.71	208	226
4	1.05	0.89	33	44	0.85	0.86	211	224
5	1.31	0.59	24	26	1.08	0.56	208	208
6	0.72	0.36	348	69	0.57	0.33	168	242

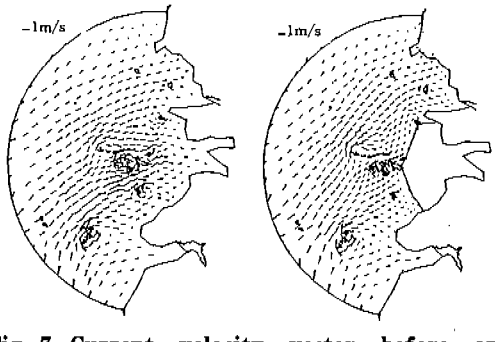

Fig. 7. Current velocity vector before and after closure at flood tide

tion pattern, it must be able to conclude there is no further changes in flow pattern due to seadike construction except the southern and northern area adjacent to the Shinsee island.

V. Conclusions

The general conclusions of this study are summarized as follows :

(1) Based upon an overall comparison of calibrated model results with available field data at 6 locations, the TIDE model behaves well and is good representation of the hydrodynamic of the Saemankeum tideland reclamation area.

(2) An inspection of the simulated tidal elevation before and after Saemankeum seadike closure shows the tendency of becoming smaller tidal ranges, however, there is no significant tidal elevation changes.

(3) The magnitude of tidal current velocity after seadike closure would become smaller than before closure in the area adjacent to the seadike during both flood and ebb tide period.

(4) The simulated overall flow pattern in a certain time shows that there is substantial changes in current velocity vectors due to seadike closure in an estuarine area.

(5) The TIDE model does an excellent job of computing the changes of tidal characteristics from resulting in seadike closure in an estuarine area.

References

1. 羅正宇, 權純國, 1995, 潮汐流動解析을 위한 非線形有限要素模型(II), 韓國農工學會誌, 第37卷, 第1號, pp. 37-48.
2. 農林水產部, 農漁村振興公社, 1995, '95 새萬金地區水理實驗 및 波浪觀測報告書.
3. Oden, J. T. and G. F. Carey, 1986, Finite Elements : Fluid Mechanics, Vol. Ⅳ, Prentice-Hall, Inc..
4. Westerink, J. J., J. J. Conner and K. D. Stolzenbach, 1988, A Frequency Time Domain Finite Element Model for Tidal Circulation Based on the Least Squares Harmonic Analysis Method, International Journal for Numerical Method in Fluids, Vol. 8, pp. 813-843.